EBioMedicine 23 (2017) 160–172

Contents lists available at ScienceDirect

EBioMedicine

journal homepage: www.ebiomedicine.com

Research Paper

Highly Selective Activation of Heat Shock Protein 70 by Allosteric Regulation Provides an Insight into Efficient Neuroinflammation Inhibition

Li-Chao Wang [a,b], Li-Xi Liao [a], Hai-Ning Lv [a], Dan Liu [c], Wei Dong [d], Jian Zhu [d], Jin-Feng Chen [a], Meng-Ling Shi [a], Ge Fu [a], Xiao-Min Song [a], Yong Jiang [a], Ke-Wu Zeng [a,**], Peng-Fei Tu [a,b,*]

[a] State Key Laboratory of Natural and Biomimetic Drugs, School of Pharmaceutical Sciences, Peking University, Beijing 100191, China
[b] State Key Laboratory of Natural Medicines, China Pharmaceutical University, Nanjing 210009, China
[c] Proteomics Laboratory, Medical and Healthy Analytical Center, Peking University Health Science Center, Beijing 100191, China
[d] State Key Laboratory of Membrane Biology, Ministry of Education Key Laboratory of Cell Proliferation and Differentiation, School of Life Sciences, Peking University, Beijing 100871, China

ARTICLE INFO

Article history:
Received 19 May 2017
Received in revised form 6 August 2017
Accepted 7 August 2017
Available online 9 August 2017

Keywords:
Heat shock protein 70 (Hsp70)
Handelin
Drug target
Covalent modification
Neuroinflammation

ABSTRACT

Heat shock protein 70 (Hsp70) is widely involved in immune disorders, making it as an attractive drug target for inflammation diseases. Nonselective induction of Hsp70 upregulation for inflammation therapy could cause extensive interference in inflammation-unrelated protein functions, potentially resulting in side effects. Nevertheless, direct pharmacological activation of Hsp70 via targeting specific functional amino acid residue may provide an insight into precise Hsp70 function regulation and a more satisfactory treatment effect for inflammation, which has not been extensively focused. Here we show a cysteine residue (Cys306) for selective Hsp70 activation using natural small-molecule handelin. Covalent modification of Cys306 significantly elevates Hsp70 activity and shows more satisfactory anti-neuroinflammation effects. Mechanism study reveals Cys306 modification by handelin induces an allosteric regulation to facilitate adenosine triphosphate hydrolysis capacity of Hsp70, which leads to the effective blockage of subsequent inflammation signaling pathway. Collectively, our study offers some insights into direct pharmacological activation of Hsp70 by specially targeting functional cysteine residue, thus providing a powerful tool for accurately modulating neuroinflammation pathogenesis in human with fewer undesirable adverse effects.

1. Introduction

Heat shock proteins (HSPs) are a family of stress response proteins found in all species exposure to stressful conditions (Kityk et al., 2012; Tsan and Gao, 2004). As a representative member of HSPs, HSP70 subfamily plays a key role in the process of protecting organisms from various stresses (Morimoto, 1998; Jäättelä, 1999; Jian et al., 2016; Yu et al., 2015). HSP70 subfamily includes Hsp70 (also called stress-inducible Hsp70), constitutively expressed heat shock cognate 70 (Hsc70), mitochondrial glucose regulating protein 75 (GRP75), and GRP78 in the endoplasmic reticulum (Jäättelä, 1999; Tsan and Gao, 2004). Hsp70 (or HSPA, encoded by the HSPA1A gene in humans) is highly expressed during cell stress and functions as an adenosine triphosphate (ATP)-dependent molecular chaperone that assists proper folding of newly synthesized proteins (Alexander and Vladimir, 1997; Gething and Sambrook, 1992). Therefore, Hsp70 is a key therapeutic target for multiple diseases.

Recently, Hsp70 has been linked to various human inflammatory diseases, including bacterial infection, colitis, autoimmune arthritis, diabetes, obesity and neurodegenerative diseases (Chung et al., 2008; Tanaka et al., 2007, 2014; Van Eden et al., 2005; Van Herwijnen et al., 2012; Van Noort, 2008). Therefore, increasing attention has been devoted to the role of Hsp70 in the process of inflammatory response. At present, Hsp70-targeted immunoregulation strategy mainly focus on upregulation of Hsp70 genetic expression at transcriptional and translational levels (Bianchi et al., 2014; Wieten et al., 2010; Yoo et al., 2000). However, Hsp70 acts as a vital signaling hub protein and is extensively involved in many physiological processes; thus nonspecific Hsp70 gene induction might cause broad disturbance of Hsp70-associated cellular signaling pathways or even undesirable adverse drug reactions. It is well known that small-molecules that target distinct protein sites can impact distinct protein functions. Therefore, investigation on direct pharmacological activation of Hsp70 by targeting specific amino acid residue in functional domain can exert a more precise regulation of

* Correspondence to: Peng-Fei Tu, State Key Laboratory of Natural and Biomimetic Drugs, School of Pharmaceutical Sciences, Peking University, Beijing 100191, China.
** Corresponding author.
E-mail addresses: ZKW@bjmu.edu.cn (K.-W. Zeng), pengfeitu@bjmu.edu.cn (P.-F. Tu).

http://dx.doi.org/10.1016/j.ebiom.2017.08.011

Hsp70 function, which leads to increased therapeutic potential and fewer side effects.

Given the importance of direct pharmacological regulation of Hsp70 in neuroinflammatory response, insights into the novel functioning regulatory site discovery are prerequisite, as they will facilitate the development of drugs for neuroinflammatory diseases. Structurally, Hsp70 is highly conserved and possesses a common domain structure composed of (i) an N-terminal nucleotide binding domain (NBD) that promotes ATP hydrolysis, and (ii) a C-terminal substrate binding domain (SBD) for substrate binding (Kityk et al., 2012; Mayer, 2013). The interdomain allostery between NBD and SBD effectuates multiple functions of Hsp70. So far no reports show effective therapeutic strategy for neuroinflammation by directly targeting specific amino acid residues on Hsp70 with chemical small-molecules.

In this study, we identify a natural small-molecule handelin as a selective Hsp70 activator to inhibit neuroinflammation. Handelin could specifically modify cysteine 306 (Cys306) of Hsp70 via the covalent Michael addition reaction, which suggests a previously unrecognized small-molecule regulatory mechanism of neuroimmunology. Further study suggests that the specific modification of handelin on Cys306 of Hsp70 causes an allosteric effect on ATP catalytic pocket to facilitate the cycle of ATP hydrolysis into adenosine diphosphate (ADP). Moreover, allosteric effect promotes Hsp70 to interact with TNF receptor-associated factor 6 (TRAF6) and further disturbs lysine 63-specific ubiquitination of TRAF6, leading to the inactivation of downstream of nuclear factor-κB (NF-κB) inflammation signaling pathway. Notably, handelin causes fewer side effects than Hsp70 gene inducer geranylgeranylacetone (GGA).

Collectively, our study identifies cysteine 306 as a druggable residue for specially activating Hsp70 to inhibit neuroinflammation, which has not been reported before. Moreover, we show a natural molecular scaffold as a selective Hsp70 activator. These results can provide some insights into the direct pharmacological regulation of Hsp70 function by targeting specific amino acid residue and also guide future rational drug design to treat human neuroimmunological diseases with fewer adverse effects.

2. Experimental Procedures

2.1. Chemicals and Reagents

Handelin ($C_{32}H_{40}O_8$; molecular weight 552.6552) was obtained from Baoji Herbest Bio-Tech Co., Ltd. (Shanxi, China) and affirmed by H^1NMR and MS data. The purity was determined to be >98% by HPLC method. Fatty acid-free bovine serum albumin (BSA) was from Equitech-Bio, Inc. (Kerrville, TX, USA). Palmitic acid (PA, TCI, Shanghai, China) was dissolved in absolute ethanol as stock solution and then conjugated with 10% BSA to achieve a concentration of 100 μM as previously described (Li et al., 2015). The recombinant human Hsp70 protein was from Sino Biological Inc. (Beijing, China).

Antibodies against iNOS (2982), COX2 (12282), GAPDH (3683), HSP70 (4873), HSC70 (8444), K63-Ubi (12930), K48-Ubi (8081), p-IKKα/β (2697), IKKα (11930), IKKβ (8943), p-IκB-α (2859), IκB-α (4814), p-NF-κB p65 (3033), NF-κB p65 (8242), HA-Tag (3724), His-Tag (2366), TRAF6 (ab94720), IL-1β (12242), TNF-α (11948), rabbit IgG (7074) and mouse IgG (7076) were purchased from Cell Signaling Technology (Beverly, MA, USA). Antibodies against Iba-1 (ab178680), CD11b/c (ab202907) and CD68 (ab31630) were obtained from Abcam Biotechnology (Cambridge, UK).

2.2. Plasmids and Cys Mutants

Human Hsp70 or TRAF6 was cloned into a pcDNA3.1 vector containing a His or HA tag sequence at the N-terminal region. Site-directed mutagenesis was performed with the QuikChange site-directed mutagenesis kit (Agilent Stratagene, La Jolla, CA, USA) using HA tag-Hsp70 as a template.

2.3. Cell Culture and Transfection

Murine BV2 microglial cell line, human embryonic kidney cell line HEK 293T and human neuroblastoma SH-SY5Y cell line were obtained from Peking Union Medical College, Cell Bank, China. All cell lines were routinely cultured in high glucose Dulbecco's Modified Eagle Medium (DMEM) with 10% heat-inactivated fetal bovine serum (FBS, PAN-Biotech, Aidenbach, Germany), 100 U/mL penicillin and 100 μg/mL streptomycin at 37 °C under 5% CO_2 atmosphere.

For siRNA knockdown studies, BV2 cells or HEK293T cells were used for Hsp70 siRNA transfection. Specific Hsp70 siRNAs were designed and synthesized at GenePharma (Jiangsu, China) as listed in Supplementary Table 1. siRNAs were premixed with lipofectamine RNAiMAX (Invitrogen®, Thermo Fisher Scientific, Waltham, MA, USA) in OPTI-medium (Gibco®, Thermo Fisher Scientific) and then applied to the cells following the manufacturer's instructions.

2.4. Determination of the Pro-Inflammatory Cytokines

BV2 cells were treated with BSA or PA for 24 h with or without handelin (0.63, 1.25 and 2.5 μM). The culture supernatants were collected and the production of NO was determined by Nitric oxide assay kit (Jiancheng Bioengineering Institute, Jiangsu, China). The levels of tumor necrosis factor α (TNF-α), interleukin 6 (IL-6) and IL-1β in the supernatants were assessed with commercial ELISA kits (ExCell Bio Company, Shanghai, China).

2.5. Detection of Microglia-Mediated Neurotoxicity

Primary cortical neurons obtained from ICR mouse embryos were cultured for 6 days as previously described (Zeng et al., 2012). BV2 cells were then seeded onto the transwell in the neurons-seeded culture wells, letting neurons and microglia share the same culture medium, but without direct contact. Microglia-neuron co-cultures were treated with PA in the presence of handelin (0.63, 1.25 and 2.5 μM) or not for 48 h. Neurons were then fixed and stained with crystal violet solution or Hoechst 33,258 solution. Images were obtained with a fluorescence microscope (IX73, Olympus, Tokyo, Japan). Moreover, neuronal viability was determined by adding 3-(4, 5-dimethyl thiazol-2-yl)-2, 5-diphenyl tetrazolium bromide (MTT) solution (Sigma-Aldrich, St. Louis, MO, USA).

2.6. Immunoblotting and Co-Immunoprecipitation (Co-IP) Analysis

Cell lysate homogenates were separated on 10% SDS-PAGE and transferred onto nitrocellulose membranes. Subsequently, the membranes were probed with specific primary and secondary antibodies. Protein bands were visualized by enhanced chemiluminescence (ECL) substrate and analyzed with Tanon 5200 Imaging Analysis System (Tanon, Shanghai, China). For Co-IP assay, cells lysates were incubated with anti-HA-tag antibody conjugated magnetic beads on ice for 4 h or anti-TRAF6 primary antibody (1:100 dilutions) and subsequent protein A + G-agarose beads for 4 h at 4 °C. The immunoprecipitated proteins were separated by SDS-PAGE and detected by immunoblotting.

2.7. RNA Extraction and Real-Time PCR Analysis

Total RNA was extracted using RNAprep pure Cell/Bacteria Kit (TianGen), and then reverse transcribed to cDNA with TIANscript RT Kit (TianGen). Quantitative real-time PCR (qRT-PCR) was conducted on Agilent Technologies Stratagene Mx3005P. The sequences of the PCR primers for each gene are described in Supplementary Table 2. The relative transcriptional level of target genes was calculated by the $2^{-\Delta\Delta CT}$ method with GAPDH as a normalizing gene (Zeng et al., 2015).

2.8. Target Protein Identification for Handelin

The handelin target proteins were pulled down according to previous report with slight modification (Liu et al., 2014). Briefly, handelin was coupled to Epoxy-activated Sepharose 6B beads (GE Healthcare, Chicago, IL, USA). The vehicle and handelin-coupled beads were subsequently mixed with cell lysates and then incubated overnight at 4 °C. The bead-captured proteins were obtained by incubating the mixture and separated to 10% SDS-PAGE, visualized by silver staining and then identified by LC-MS/MS using a nano-HPLC-tandem LTQ-Orbitrap Velos pro mass spectrometer (Thermo Fisher Scientific) as our previous study reported (Liao et al., 2017).

2.9. Surface Plasmon Resonance (SPR) Assay

Interaction between handelin and Hsp70 was quantitatively analyzed using the Biacore T200 system (GE Healthcare). The purified recombinant human Hsp70 protein (500 μg/mL) was immobilized on a carboxymethylated 5 sensor chip using a standard amine coupling method. Gradient concentrations of handelin (0.04 to 50 μM) in the running buffer were injected as analytes. Data were analyzed with the Biacore evaluation software (T200 Version 2.0) and fitted to a 1:1 Langmuir model to give results. The kinetic parameters of K_a, K_d and K_D were derived by fitting to a 1:1 Langmuir binding model.

2.10. Cellular Thermal Shift Assay (CETSA)

For the living cell CETSA experiments (Lomenick et al., 2011), BV2 cells were treated with handelin at 2.5 μM for 2 h, and then heated individually at indicated temperatures for 3 min followed by cooling at room temperature. The cells were collected and freeze-thawed five times using liquid nitrogen. The lysates were then analyzed by SDS-PAGE followed by immunoblotting for Hsp70.

For the cell lysate CETSA experiments, BV2 cells were freeze-thawed five times using liquid nitrogen. The cell lysates were divided into two aliquots, with one aliquot served as control and the other being incubated with handelin (10 μM) for 1 h at room temperature. The lysates were then heated and analyzed for Hsp70 in the same manner.

2.11. Drug Affinity Responsive Target Stability (DARTS) Assay

BV2 cell lysates were incubated with different concentrations of handelin for 1 h followed by addition of 5 μg/mL pronase for a further 15 min at room temperature (Molina et al., 2013). Reactions were ceased by adding the SDS-PAGE loading buffer and analyzed by immunoblot with a specific anti-Hsp70 antibody.

2.12. NF-κB Reporter Assay

A NF-κB-luciferase reporter gene stably expressed BV2 cell line (NF-κB-luc-BV2) was generated by transfecting NF-κB target sequence linked-luciferase reporter plasmid with lipofectamine 2000 transfection reagent. NF-κB-luc-BV2 cells were treated with PA in the absence or the presence handelin (0.63, 1.25, and 2.5 μM) for 8 h, and then analyzed for luciferase activity using a luciferase reporter gene assay kit (Bioassay sys, Hayward, CA, USA) on a fluorescence spectrophotometer (PerkinElmer, Waltham, MA, USA).

2.13. Identification of GSH-Handelin Complex by LC-MS

Glutathione (GSH, 500 μM) was incubated with handelin (500 μM) for 2 h at 37 °C. Then, the GSH-handelin complex was analyzed by liquid chromatography coupled with hybrid triple quadrupole-linear ion trap mass spectrometer (LC-Q-trap-MS) method. The protocol was according to previous report (Liao et al., 2017) excepting that the mobile phase consisting of water (0.1% formic acid, A) and acetonitrile (B), was delivered at a constant flow rate of 0.4 mL/min with a gradient elution of 5–20% B at 0–1 min, 20–100% B at 1–3 min.

2.14. Determination of Handelin-Binding Site on Hsp70

Recombinant Hsp70 protein was incubated with handelin for overnight at 4 °C, and the mixture was purified using an ultrafiltration tube. For the identification of handelin-binding site on Hsp70, the nano-LC-MS/MS experiments were performed using an EASY-nLC II system and a LTQ-Orbitrap velos pro mass spectrometer according to our previous study (Liao et al., 2017). Mass spectrometric data were analyzed with Proteome Discoverer (1.4) software with the SEQUEST search engine (Thermo Fisher Scientific) using the following criteria: taxonomy, human; enzyme, trypsin; missed cleavage sites, 2; variable modifications, methionine oxidation (+15.995 Da), cysteine carbamidomethylation (+57.021 Da), cysteine binding with Hsp70 (+552.272 Da); precursor mass tolerance as 10 ppm, fragment mass tolerance as 0.6 Da; and the false discovery rate (FDR) at 0.01.

2.15. In Vitro Hsp70 ATPase Activity Assay

Recombinant human Hsp70 protein solution was preincubated with various concentrations of handelin for 30 min, and then incubated with 2.5 mM ATP for 3 h at 37 °C. The malachite green based colorimetric assay was adopted from previous report (Ko et al., 2015) to afford the inorganic phosphate concentration, which was calculated by calibrating the concentration from a sodium phosphate standard curve. The ADP level was detected using a commercial ADP colorimetric assay kit II (Sigma-Aldrich). Relative inorganic phosphate or ADP was expressed as a fold change over the control.

2.16. Tryptophan Fluorescence Quenching Study

The recombinant human Hsp70 protein was incubated with handelin (0.5–50 μM) or vehicle in a quartz plate. Tryptophan fluorescence spectra of the initial protein and those upon a successive addition of handelin solutions were recorded. Fluorescence was detected by setting excitation wavelength at 280 nm and emission wavelengths from 300 to 550 nm at 1 nm increment on a fluorescence spectrophotometer (PerkinElmer). The fluorescence intensities were corrected by the buffer contribution.

2.17. Molecular Dynamics Simulations and Analyses

2.17.1. System Setups

The initial models of human heat shock 70 kDa protein 1A/B protein the in an open state and in a closed state were generated by homology modeling based on the templates Human Hsp70 Chaperone BiP (PDB ID code: 5E84, chain A) and *E. coli* DnaK (PDB ID code: 2KHO, chain A) from the PDB database, respectively. Four series of systems were designed: the Hsp70 in a low affinity open state binding with or without handelin and the Hsp70 in a high affinity closed state binding with or without handelin. Geometry optimization and the electrostatic potential calculations were carried out at the HF/6-31G/ level of Gaussian09 suite. The force field parameters for handelin covalently bonded to Cys306 residue of Hsp70 protein were generated by the General AMBER Force Field (GAFF) and Restrained Electrostatic Potential (RESP). The resulting structures were solvated using the explicit TIP3P water box with a distance of 10 Å between protein surface and the solvation boundary and neutralized by adding Na^+ counter ions.

2.17.2. Model Building and Molecular Dynamics (MD) Simulation

All-atom MD simulations were then carried out using Amber14 package, employing the AMBER 14 gaff and ff14SB force fields. The simulation protocol included standard steps of energy minimization, gradually heating from 0 to 300 K in NVT ensemble and equilibrated at

pressure of 1 atm in NPT ensemble. During the simulations, the periodic boundary conditions were employed and interactions between atoms were truncated with a cutoff radius of 1.0 nm for van der Waals and Coulomb using Particle-mesh Ewald (PME) for the long-term electrostatic treatment. All the covalent bonds involving hydrogen atoms were constrained with the SHAKE algorithm. MD simulations production continued 100 ns without any constraints in the NPT ensemble at a temperature of 300.0 K and a pressure of 1 atm. Production snapshots were recorded every 1 ps.

2.18. Immunofluorescent Colocalization Analysis

HEK293T cells were transiently co-transfected His-tagged Hsp70 and HA-tagged TRAF6 plasmids using lipofectamine 2000 transfection reagent and then treated with or without 2.5 μM hadelin for 6 h. Cells were incubated with mixed His-tag mouse primary antibody and HA-tag rabbit primary antibody followed by adding a mixture of Alexa Fluor 594-labeled anti-rabbit and Alexa Fluor 488-labeled anti-mouse secondary antibody. After being stained with DAPI, the cells imaged by confocal microscopy (Leica TCS SP8 X, Leica Microsystems, Wetzlar, Germany).

2.19. Animal Studies

Male BALB/c mice (6–8 weeks old, 18–22 g) were obtained from Vital River Company (Beijing, China). Animals were maintained under 12 h light/dark cycle at 25 ± 2 °C with free access to water and standard diet (SD). The procedures for daily animal care and experiments were conducted in accordance with 'The Detailed Rules and Regulations of Medical Animal Experiments Administration and Implementation' (Document no. 1998-55, Ministry of Public Health, China), and were approved by Institutional Animal Care and Use Committee of Peking University (License No. LA2016318).

For the high-fat diet (HFD) mouse model challenge, BALB/c mice were fed a HFD containing 10% lard, 10% yolk, 1% cholesterol, 0.2% cholate and 78.8% standard diet for 14 days. Mice received gavage administration of 0.5% CMC-Na solution in control and model groups, and handelin (10 or 20 mg/kg/day) in therapy groups since day 8. After being fasted for 8 h, mice were sacrificed with decapitation and the brains were removed. Immunoblotting assay and immunohistochemistry assay were performed with specific antibodies for detecting the microglia activation in brain.

BALB/c mice received gavage administration of 0.5% CMC-Na solution, handelin or GGA (100 mg/kg/d) for three consecutive days.

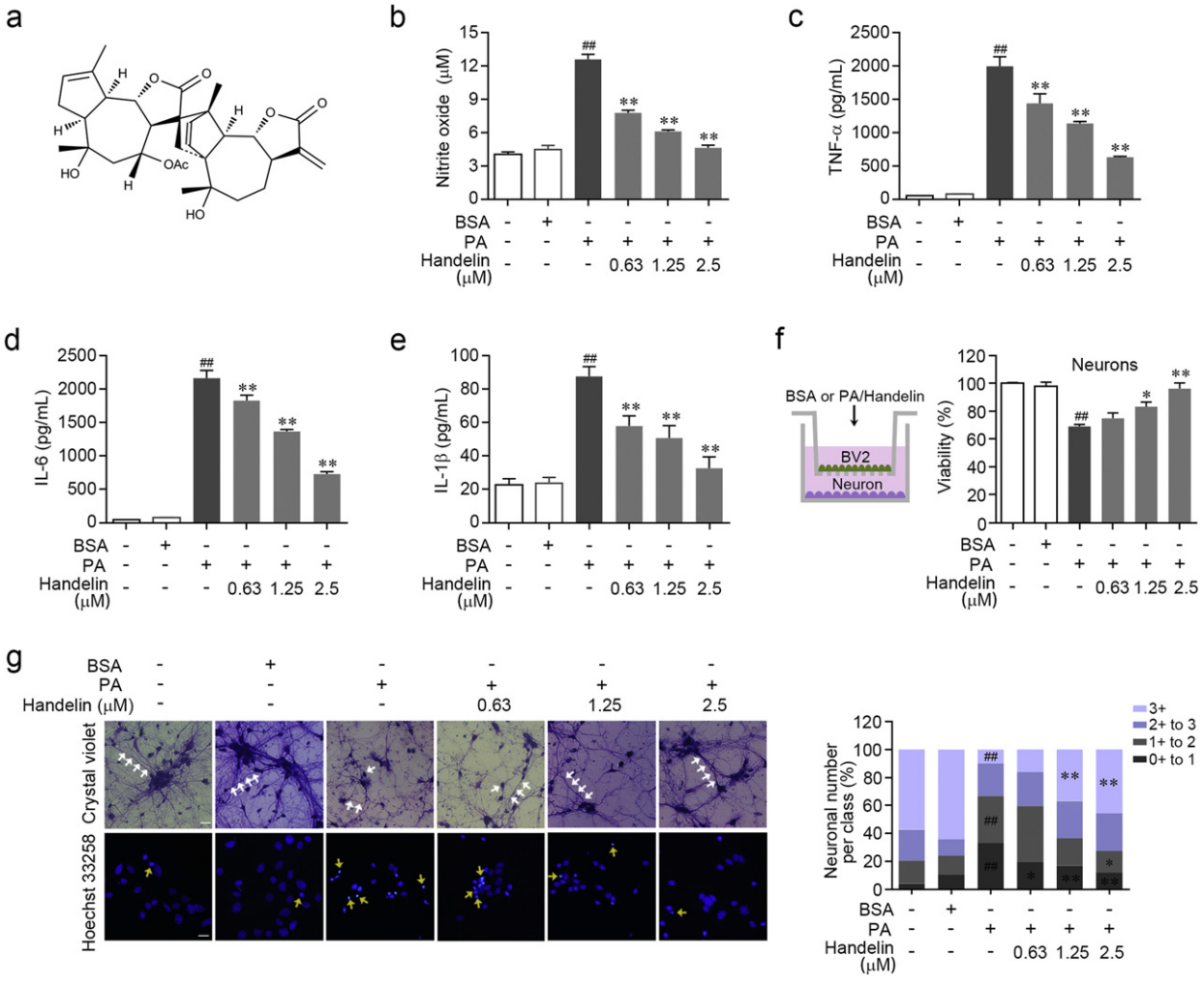

Fig. 1. Handelin exerts anti-neuroinflammation and neuroprotection. (a) Chemical structure of handelin. (b)–(e) BV2 cells were treated with 10% BSA or PA (100 μM) in the presence of handelin at concentrations shown for 24 h. Then the levels of NO (b), TNF-α (c), IL-6 (d) and IL-1β (e) were detected by Griess and ELISA assay. (f)–(g) Microglia-neuron co-cultures were incubated with BSA, PA or/and handelin for 48 h. Then, neurons were tested for MTT assay (f), stained with crystal violet and Hoechst 33,258 solution (g), respectively. Typical morphological changes of neurons marked by white arrows were classified into 4 subtypes (0 to 3+) according to the ratio of neurite length and cell body diameter and statistically analyzed. Typical apoptotic neurons were labeled with yellow arrows. Scale bar represents 20 μm. Data are expressed as mean ± SEM for three individual experiments. $^{*}P < 0.05$, $^{**}P < 0.01$, vs. PA group. $^{\#\#}P < 0.01$ vs. control group.

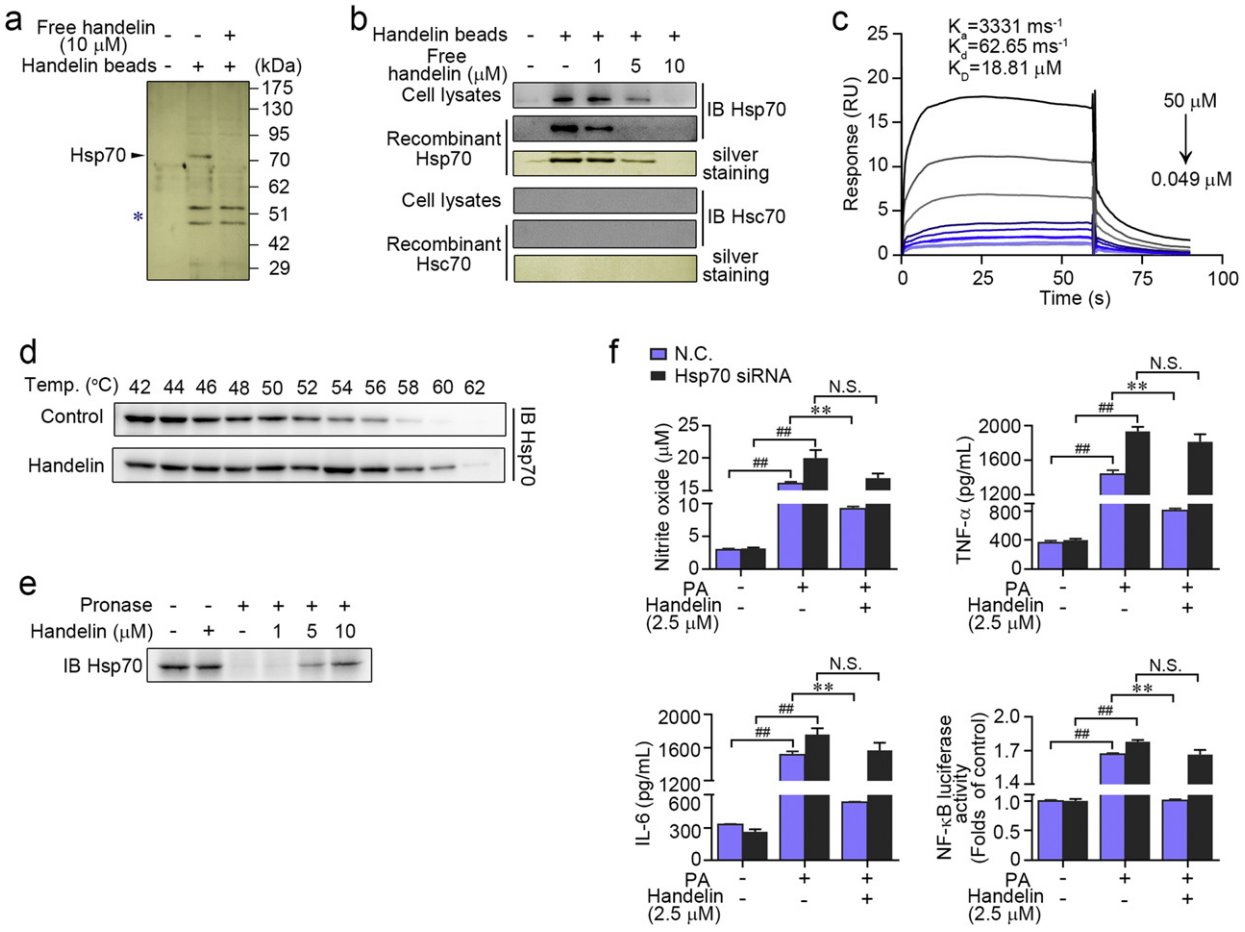

Fig. 2. Identification of Hsp70 as a molecular target for handelin. (a) Handelin-conjugated sepharose beads were incubated with BV2 cells lysates in the presence or absence of excess handelin (10 μM). The intense ~70 kDa band was excised from the gel and identified as heat shock protein 70 (Hsp70). The asterisk marked bands indicated nonspecific beads-bound vimentin and actin. (b) Handelin-conjugated beads were incubated with cell lysates or a recombinant Hsp70 (or Hsc70) protein and handelin at concentrations shown, and then the proteins bound to the beads were detected by immunoblotting and silver staining. (c) Representative graph of surface plasmon resonance spectroscopy analysis showing the kinetics of increasing concentrations of handelin binding to human recombinant Hsp70. The kinetic parameters of K_a, K_d, and K_D were derived by fitting to a 1:1 Langmuir binding model. (d) BV2 cells were exposed to handelin (10 μM) or vehicle followed by a cellular thermal shift assay. (e) BV2 cell lysates was incubated with handelin in the presence or absence of pronase (5 μg/mL). (f) Reverse effects of Hsp70 gene silence on handelin-mediated inhibition of nitrite oxide, TNF-α, IL-6 and NF-κB luciferase activity. Data are expressed as mean ± SEM for three individual experiments. $^{*}P < 0.05$, $^{**}P < 0.01$ vs. PA group. $^{\#\#}P < 0.01$ vs. control group. N.S., not significant.

Routine peripheral blood cells were analyzed by using a celltac α MEK-6400 automated hematology system (Nihon Kohden, Tokyo, Japan). Serum total cholesterol (TC) levels were measured using a commercial available assay kit (Jiancheng Bioengineering Institute).

2.20. Heat Shock Injury

SH-SY5Y cells were exposed to heat shock at 45 °C for 20 min and recovered at 37 °C for indicated time. Cell viability was determined by MTT assay. To evaluate Hsp70 expression, the cells were harvested, lysed and analyzed by immunoblotting with a specific anti-Hsp70 antibody.

2.21. Caenorhabditis elegans Lifespan Assay

The *Caenorhabditis elegans* strain N2 was grown on NGM (normal growth medium) agar plates seeded with *Escherichia coli* OP50 bacterial lawns. Worms at L4 larval stage were cultured on fresh plates containing 50 μM handelin or vehicle. The lifespan were monitored by examining the survival of animals every two days. Worms failed respond to gentle prodding with movement were scored as dead. All lifespans were plotted with L4 as time-point 0.

2.22. Zebrafish Embryos Development Experiment

Wild-type Tübingen zebrafish (*Danio rerio*) strain was raised under standard conditions. Normal fertilized WT embryos were collected and cultured in the Petri dish with egg water. The healthy embryos at 24 h pose fertilization (hpf) were treated with 30 μM handelin or vehicle. After 72 hpf, the living embryos were counted for statistical analysis.

2.23. Statistical Analysis

All data were expressed as means ± SEM (standard error of the mean), with *n* representing the number of independent experiments. GraphPad Prism 6.0 was used for statistical analysis and graphs. Mean values were compared by one-way analysis of variance (ANOVA) with Dunnett's *post-hoc* test. $P < 0.05$ was considered as statistically significant.

3. Results

3.1. Anti-Neuroinflammation Small-Molecule Probe Discovery

In this study, we established a palmitic acid (PA)-induced microglia-based anti-neuroinflammation screening model for discovering small-

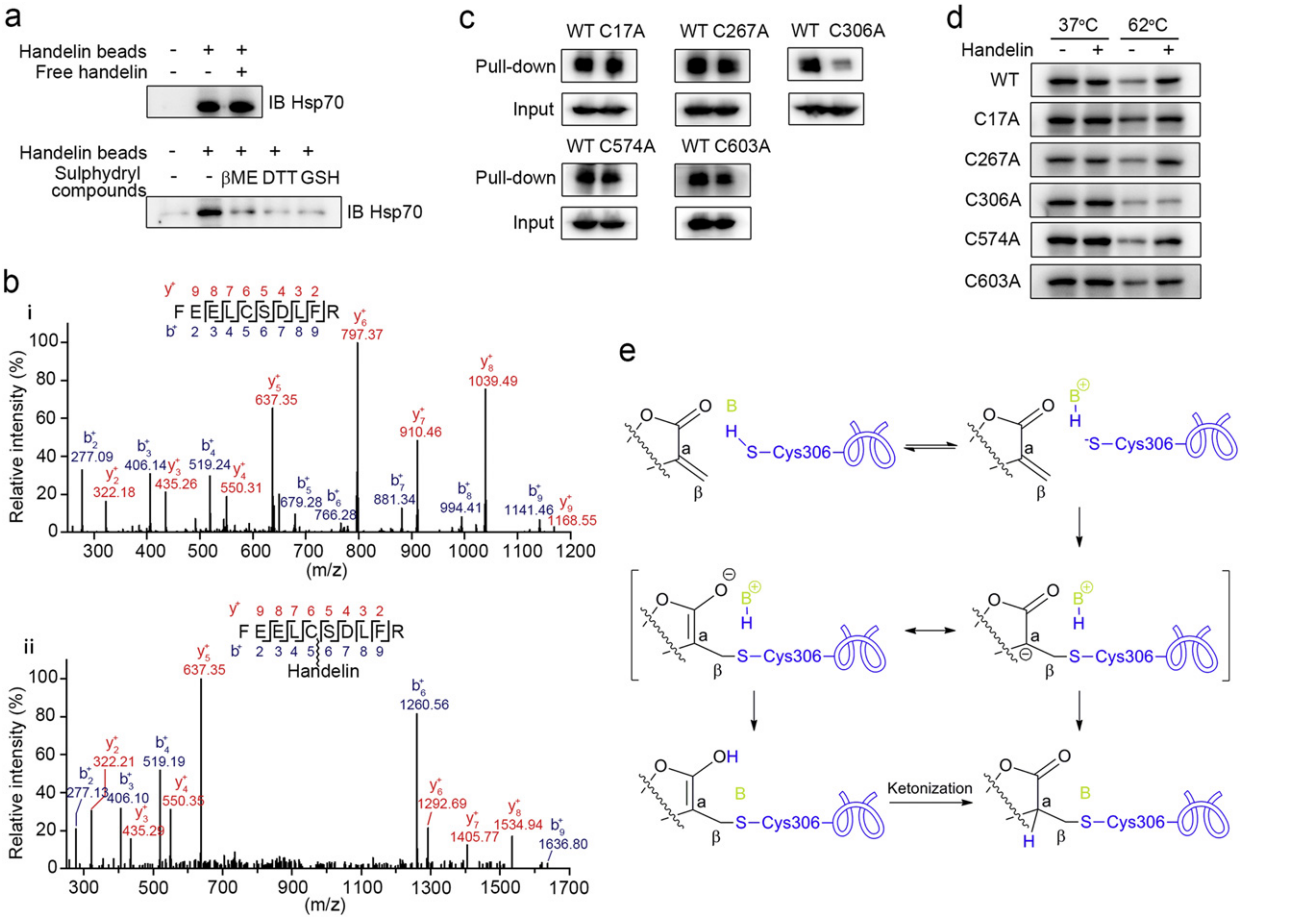

Fig. 3. Handelin covalently binds to Cys306 residue. (a) Handelin beads were incubated with BV2 cells lysates containing sulphydryl compounds or not as indicated. In post-treatment group, handelin at 10 μM was added and incubated for another 12 h. The beads-bound protein was analyzed by immunoblotting. (b) LC-MS/MS analysis of the recombinant Hsp70 protein incubated without (i) or with (ii) handelin. (c)–(d) HEK293T cells were transfected with wild-type or cysteine-mutant HA-Hsp70 plasmids. Cells were lysed to pull-down with handelin-conjugated sepharose beads (c) or exposed to handelin (10 μM) followed by a cellular thermal shift assay (d). (e) The proposed covalent binding mode of handelin with Hsp70.

molecule probes. In our previous activity screening experiment, we tested 1150 small-molecule compounds in our natural chemical library and identified handelin (Fig. 1a, Kang et al., 1996) as a potent anti-neuroinflammatory candidate probe. We found handelin potently blocked PA-induced nitrite oxide release in a concentration-dependent manner (IC_{50} 0.87 μM), but without any toxicity (Fig. 1b and Supplementary Fig. 1a–b). Moreover, the secretions of various proinflammatory cytokines including TNF-α, IL-6 and IL-1β were significantly inhibited by handelin treatment (Fig. 1c–e), as well as the corresponding inflammatory gene expressions (Supplementary Fig. 1c). Furthermore, the inhibitory effect of handelin on neuroinflammation was confirmed by significant down-regulation of inducible nitric oxide synthase (iNOS) and cyclooxygenase 2 (COX2) protein expressions (Supplementary Fig. 1d).

To explore whether handelin-dependent neuroinflammation suppression could lead to effective neuroprotection, neuron-microglia co-cultures were established in vitro. In cortical neuron alone cultures, neither handelin nor PA showed any cytotoxic effect (Supplementary Fig. 1e and f). However, in microglia-neuron co-cultures, PA caused a significant decrease of neuronal viability through promoting neurotoxic inflammatory mediators release from microglia, which was effectively antagonized by handelin (Fig. 1f). In addition, morphological observation revealed that handelin markedly protected the integrity of neuronal synaptic connections and prevented neuron apoptosis against microglia-mediated neurotoxicity (Fig. 1g). These results indicate that handelin is a potent small-molecule inhibitor against microglia-mediated neuroinflammation as well as neurotoxicity.

3.2. Handelin Directly Targets Hsp70

To elucidate the direct cellular targets of handelin, we prepared handelin-conjugated sepharose beads as affinity reagent based on previous report (Liu et al., 2014). BV2 cell lysates were incubated with handelin-conjugated sepharose beads to capture the target proteins, and then the proteins specifically bound to handelin-conjugated sepharose beads were resolved by SDS-PAGE and stained with silver. An obvious protein band at ~70 kDa was identified as Hsp70 by liquid chromatography combined with LTQ-Orbitrap Velos pro mass spectrometry (LC-MS/MS) analysis (Fig. 2a, Supplementary Fig. 2a and b). In particular, no obvious protein band was found in control group or the group with an excess amount of handelin competition, indicating the specificity of handelin binding to Hsp70 (Fig. 2a). We next tried to evaluate the selectivity of handelin binding between different HSP70 family isoforms including Hsp70 and Hsc70. As shown in Fig. 2b, both recombinant and cell endogenous Hsp70 were pulled down by handelin-conjugated sepharose beads, which was concentration-dependently reversed by excess amount of handelin competition, indicating a specific association of handelin to Hsp70. Moreover, we incubated recombinant Hsc70 protein or cell lysate with handelin-conjugated sepharose beads; however, no specific Hsc70 protein band was detected, confirming a selective interaction of handelin with Hsp70 but not Hsc70 (Fig. 2b). We further quantitatively investigated the interaction of handelin with Hsp70 using surface plasmon resonance (SPR) technology. As shown in Fig. 2c, handelin specifically bound to Hsp70 in a

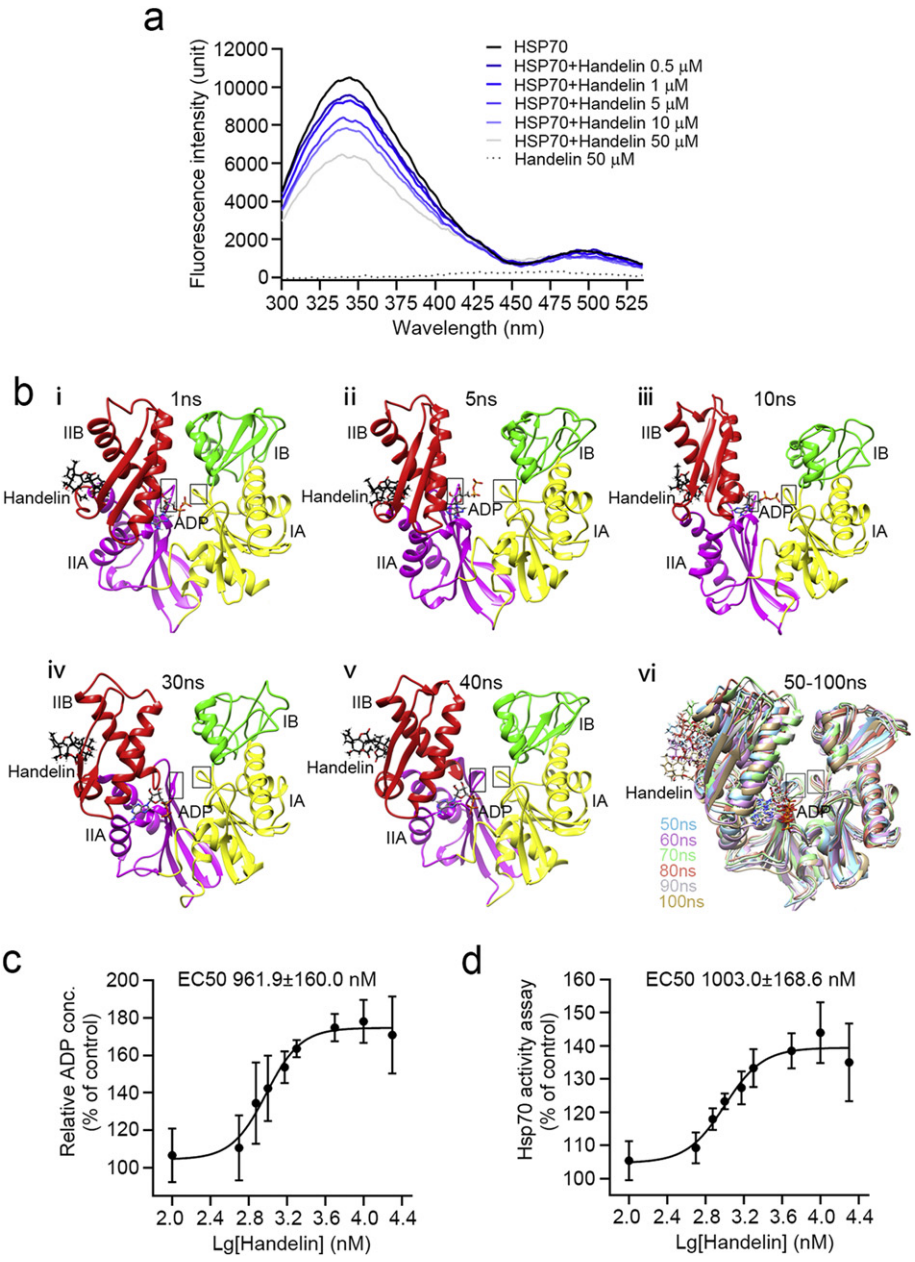

Fig. 4. Handelin activates Hsp70 by allosteric effect. (a) Fluorescence spectroscopy analysis of the interaction of Hsp70 with handelin. Fluorescence for recombinant human Hsp70 protein treated or untreated with various concentrations of handelin was collected. (b) Representative conformations of NBD (ADP) in handelin bound Hsp70 system obtained by 100 ns of MD simulations using Amber14. (c) Effects of handelin on the ADP of Hsp70 measured using a colorimetric assay. (d) Effects of handelin on the ATPase activity of Hsp70 measured using a malachite assay.

concentration-dependent manner with dissociation constants (K_D) of 18.81 μM, indicating a strong binding capacity of handelin to Hsp70.

We next aimed to monitor drug target engagement in cells via cellular thermal shift assay (CETSA) and drug affinity responsive target stability (DARTS) assay. CETSA showed that handelin significantly increased the stability of Hsp70 compared with the vehicle group both in situ BV2 cells and cell lysate (Fig. 2d and Supplementary Fig. 2c). In addition, handelin concentration-dependently inhibited protease

Fig. 5. The HSP70-TRAF6 axis is responsible for handelin-dependent neuroinflammation inhibition. (a) HEK293T cells transfected with HA-tagged Hsp70 vector treated by 2.5 μM handelin or vehicle. Co-immunoprecipitation (Co-IP) was performed with an anti-HA antibody followed by immunoblotting with indicated antibodies. (b) HA-TRAF6 over-expressed HEK293T cells were treated by 2.5 μM handelin or vehicle, and then subjected to CO-IP with anti-HA antibody followed by silver staining. The band at about 70 kDa was identified as Hsp70 by MS analysis. The asterisk marked bands indicated nonspecific beads-bound actin. (c) Handelin-conjugated beads were incubated with BV2 lysates and handelin at concentrations shown. The beads-bound proteins were washed by 1% NP40- or SDS-contained buffer, followed by immunoblotting for Hsp70 and TRAF6. (d) Handelin-conjugated beads were incubated with HA-TRAF6 protein and handelin at concentrations shown. The proteins bound to the beads were analyzed by immunoblotting for HA. (e) HA-TRAF6 transfected HEK293T cells were harvested and lysed, followed by IP with anti-HA antibody. The precipitate was further incubated with purified recombinant Hsp70-His protein containing handelin or not. Immunoblotting was employed for His and HA. (f) Colocalization of HA-tagged TRAF6 (red) with His-tagged Hsp70 (green). Scale bars = 25 μm. (g) BV2 cells were treated with PA and handelin. Co-IP and immunoblotting were performed with indicated antibodies. (h) HEK293T cells co-transfected with HA-TRAF6 vector and siRNA duplexes specific for Hsp70 were treated with 2.5 μM handelin or vehicle. Co-IP and immunoblotting were then performed. (i) Effects of handelin on PA-induced NO, TNF-α and IL-6 production and cell viability in mock- or TRAF6-transfected BV2 cells. Data are expressed as mean ± SEM for three individual experiments. $^{*}P$, $^{\$}P < 0.05$; $^{\#\#}P$, $^{**}P$, $^{\$\$}P < 0.01$; N.S., not significant.

induced-degradation of Hsp70, supporting the direct interaction of handelin with Hsp70 (Fig. 2e).

Inducible Hsp70, the major heat shock protein thought to protect cells from a variety of diseases, has been widely reported to be involved in inflammation activation. Here, we attempted to explore its role in handelin-mediated neuroinflammation suppression using specific Hsp70 gene silenced-BV2 cells. As shown in Fig. 2f, handelin-dependent anti-neuroinflammation effects were markedly reversed by specifically

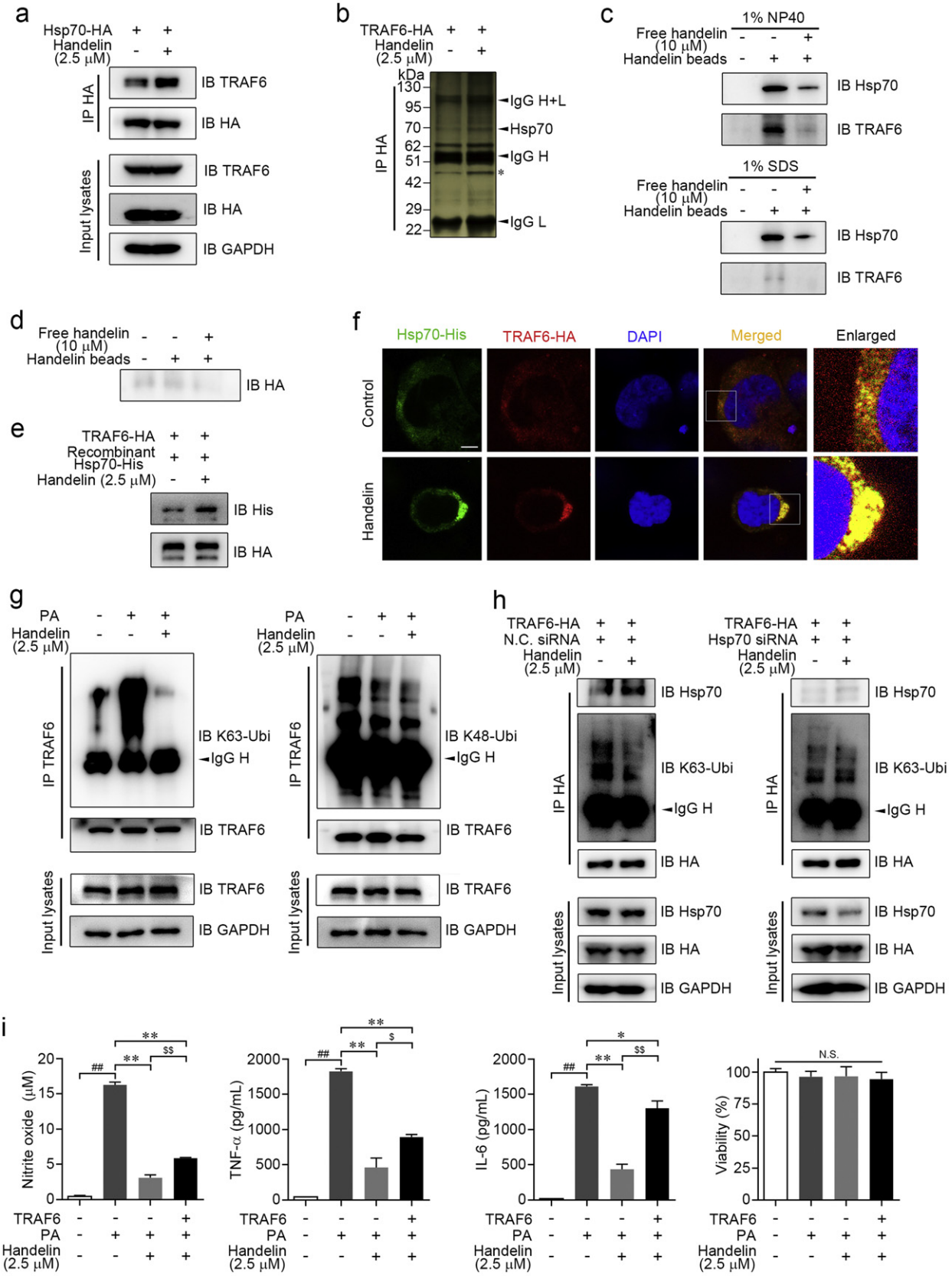

knocking down Hsp70 gene expression, suggesting that Hsp70 acts as a key cell target responsible for handelin-mediated anti-inflammatory effect.

3.3. Cysteine 306 is Covalently Modified by Handelin

To pinpoint the property of handelin interacting with Hsp70, we firstly tested whether handelin could covalently bind to Hsp70. Handelin-conjugated sepharose beads were pre-incubated with BV2 cell lysates, and then further treated with an excess amount of handelin as competition. As shown in Fig. 3a, post-competition of handelin failed to prevent Hsp70 binding to the beads. Thus we speculated that there might be a covalent bond formation between handelin and Hsp70. Notably, handelin contains α, β-unsaturated carbonyl group which possesses the potential to react covalently with the sulphydryl of cysteine on Hsp70 (Nilsson et al., 2001). We then detected the influences of several agents with sulphydryl including β-mercaptoethanol (βME), dithiothreitol (DTT) and glutathione (GSH) on the association of Hsp70 with handelin-conjugated sepharose beads. To our surprise, all the sulphydryl agents completely abolished the capacity of Hsp70 binding to the beads (Fig. 3a), suggesting that handelin might covalently bind to the sulphydryl of cysteine on Hsp70. To clarify the detailed interaction mode of handelin with sulphydryl, we further incubated handelin with GSH, a basic peptide with sulphydryl, and identified the products via LC-MS/MS analysis. The result successfully validated the addition reaction between the α, β-unsaturated carbonyl group of handelin and sulphydryl (handelin-GSH complex) by mass fragmentation pathway interpretation (Supplementary Fig. 3a).

There are five cysteine residues in Hsp70. Therefore, to ascertain which cysteine residue was modified by handelin, we introduced an LC-MS/MS analysis following the incubation of recombinant Hsp70 protein with handelin. Data analysis of tryptic reaction products identified a peptide (FEELCSDLFR) with a calculated mass of 1810.86 Da, which is 552.28 Da larger than the corresponding peptide in recombinant Hsp70 with a calculated mass of 1258.58 Da (Fig. 3b). The mass difference of 552.28 Da exactly matches the molecular weight of a handelin, suggesting the peptide FEELCSDLFR in Hsp70 was specifically modified by handelin. Moreover, MS/MS spectrometry of this peptide revealed that a 552.28 Da mass shift occurred starting from b4 to b5 fragment ions, indicating the cysteine in this peptide (corresponding Cys306 in Hsp70) was modified by handelin. To further validate this observation, we incubated the synthetic peptide derived from human Hsp70 containing Cys306 (PeptideC306, FEELCSDLFR) with handelin, and the same mass shift behavior for peptide C306 was confirmed by the LC-MS/MS analysis (Supplementary Fig. 3b). These findings show that the Cys306 residue of Hsp70 is covalently modified by handelin.

To map the functional significance of Cys306 for binding with handelin, we mutated all the cysteine residues in Hsp70 into alanine, respectively. Of note, pull-down assays with recombinant cysteine-mutated Hsp70 showed that only Cys306 mutation abolished the capacity of Hsp70 binding to handelin, indicating that handelin interacts with Hsp70 via selective modification of Cys306 residue (Fig. 3c). Similarly, CETSA assays with recombinant cysteine-mutated Hsp70 further supported our finding that handelin covalently integrated to Cys306 in Hsp70 (Fig. 3d). Overall, it suggests that handelin directly targets the Cys306 of Hsp70 protein via the Michael addition of sulphydryl in cysteine to the α, β-unsaturated carbonyl (Fig. 3e).

3.4. Handelin Activates Hsp70 by Allosteric Effect

Hsp70 consists of two main domains, connected by a flexible hydrophobic linker: an N-terminal nucleotide binding domain (NBD) that harbors ATPase activity and a C-terminal substrate binding domain (SBD) that recognizes polypeptide substrates. NBD catalyzes ATP hydrolysis to ADP by its ATP catalytic pocket and renders conformational changes in the adjacent SBD that enhance the affinity for substrates (Ko et al., 2015; Mayer, 2013). Handelin covalently binds to Cys306 in NBD which locates in ATP catalytic pocket, thus it is of great interest to know whether handelin affects ATP hydrolysis and Hsp70 conformations. We first conducted fluorescence analysis of tryptophan in Hsp70 to investigate the role of handelin in the regulation of Hsp70 conformation. As shown in Fig. 4a, the fluorescence intensity of handelin-Hsp70 complex decreased as handelin concentration increased. The maximum wavelength of emission spectra was blued-shifted at 50 μM of handelin. These observations reveal that handelin could induce Hsp70 conformation changes.

We next performed molecular dynamics simulation (MD) to dissect the allosteric mechanism of Hsp70. There are two main conformations for Hsp70: the low affinity open state (with ATP bound to NBD) and high affinity closed state (with ADP bound to NBD). In closed state, ADP is initially embedded in the deep cleft between NBD subdomain lobe I and lobe II. Upon handelin binding to Cys306, the two lobes in NBD are gradually separated thus enabling ADP move out of NBD, giving rise to an accelerated circulation of ATP hydrolysis (Fig. 4b and Supplementary Fig. 4a). To confirm this mechanism, we determined the level of free ADP in handelin-treated Hsp70 together with ATP as substrate, and found an obvious promoting effect of handelin on the release of ADP (EC_{50} 0.96 μM), a key product of ATPase-catalyzed hydrolysis reaction (Fig. 4c). In open state, ATP disassociates from the subdomain lobe IB and tightly interacts with hydrophilic residues threonine 13 (Thr13) and Thr14 in subdomain lobe IA via hydrogen bonds (Supplementary Fig. 4b and c). Compared to the vehicle ATP-bound Hsp70, handelin had no obvious regulation effects on the association of ATP with these hydrophilic residues which facilitate the ATP hydrolysis through promoting phosphate group release (Supplementary Fig. 4b and c). Interestingly, the malachite green assay, a colorimetric method used to monitor inorganic phosphate concentration, revealed that handelin significantly increased the level of monophosphate release from ATP in a concentration-dependent manner with an EC_{50} at 1.03 μM (Fig. 4d). Collectively, these data suggest that handelin elevated ATPase activity of Hsp70 with allosteric effect in the closed state.

3.5. Hsp70 Activation Exerts Anti-Neuroinflammation Through Regulating TRAF6 Ubiquitination

We next investigated the role of Hsp70 in handelin-dependent neuroinflammation inhibition. Hsp70 has been reported to exert negative effect on inflammation response by interfering TRAF6 ubiquitination (Chen et al., 2006). In this study, we observed handelin obviously enhanced Hsp70-TRAF6 interaction by Co-IP assay (Fig. 5a, b, Supplementary Fig. 5a and b). Moreover, we explored the interaction between handelin and TRAF6 by pull-down experiments. As shown in Fig. 5c, both TRAF6 and Hsp70 were pulled down by handelin-conjugated sepharose beads using Nonidet P40 (NP40)-contained washing buffer. However, TRAF6 could not be pulled down using sodium dodecyl sulfonate (SDS)-contained washing buffer (Fig. 5c). Because SDS is a strong detergent which could destroy protein-protein interaction, we then speculated that handelin might not directly target TRAF6. This was also supported by the finding that the TRAF6 protein could not bind to handelin-conjugated sepharose beads by immunoblotting analysis (Fig. 5d). Therefore, these observations suggest that handelin regulates Hsp70-TRAF6 complex via directly targeting Hsp70, but not TRAF6. Further determination of Hsp70-TRAF6 complex formation in overexpressed cells also demonstrated handelin directly enhanced Hsp70-TRAF6 interaction (Fig. 5e). Moreover, we observed an enhanced colocalization of Hsp70 and TRAF6 in HEK293T cells (Fig. 5f). Taken together, these results indicate that handelin directly binds to Hsp70 to facilitate Hsp70-TRAF6 interaction.

TRAF6 possesses the ubiquitin E3 ligase activity to catalyze autopolyubiquitination of itself, among which lysine 48 (K48)- and lysine 63 (K63)-linked polyubiquitination are the two most abundant types (Mishima et al., 2015; Zeng et al., 2015). K48-linked

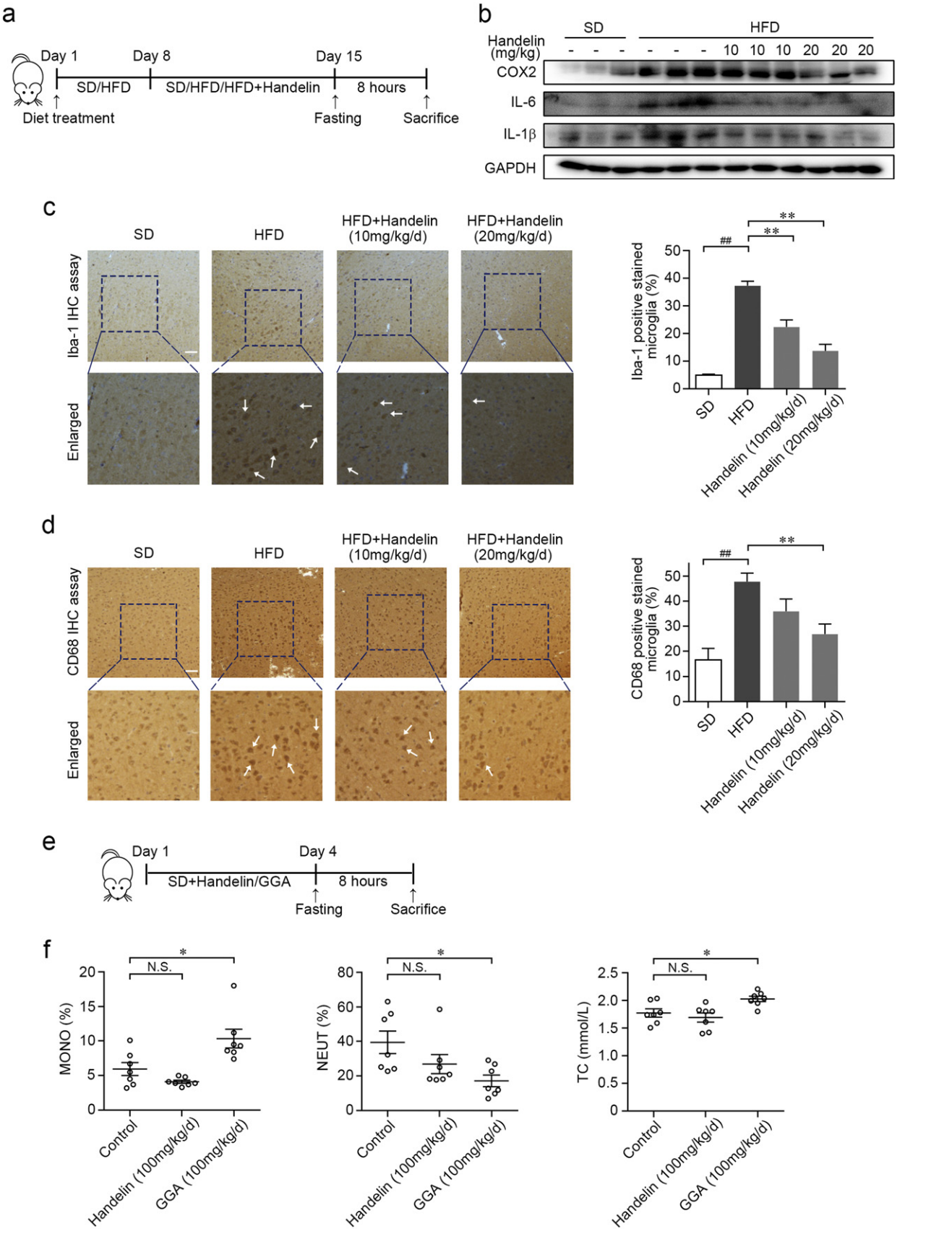

Fig. 6. Handelin inhibits neuroinflammation in HFD-induced mouse model. (a) Scheme of the HFD model. (b) Differential inflammatory protein expressions in the brains were measured by immunoblotting. (c–d) Representative images of cerebral cortex stained with the specific microglia marker Iba-1 (c) and CD68 (d). Arrows indicate the positive stained microglia. (e) Scheme of the handelin and GGA administration. (f) Effects of handelin and GGA on serum total cholesterol (TC), neutrophils ratio (NEUT%) and monocytes ratio (MONO%). Data are expressed as mean ± SEM for three individual experiments. $^{*}P < 0.05$; $^{**}P$, $^{\#\#}P < 0.01$; N.S., not significant.

polyubiquitination is responsible for proteasome-dependent TRAF6 protein degradation, whereas K63-linked polyubiquitination activates TRAF6-associated inflammatory signaling pathways (Mishima et al., 2015; Zeng et al., 2015). Then, we checked whether handelin-mediated Hsp70-TRAF6 interaction could affect K48- and/or K63-linked TRAF6 ubiquitination. We found that handelin abrogated K63-linked polyubiquitin chain formation on TRAF6, but without any effect on K48-linked polyubiquitin chain formation (Fig. 5g). Meanwhile, TRAF6 protein and relative mRNA levels remained unchanged (Supplementary Fig. 5c and d). We further explored whether Hsp70 was involved in handelin-mediated suppression of K63-polyubiquitination on TRAF6. As shown in Fig. 5h, K63-polyubiquitin expression on TRAF6 was significantly decreased by handelin; however, knockdown of Hsp70 markedly antagonized handelin-mediated deubiquitination effect on TRAF6. Therefore, these findings indicate that handelin could promote Hsp70-TRAF6 interaction which leads to the inhibitory effect on K63-linked polyubiquitination on TRAF6. Besides, the Hsp70-mediated neuroinflammation inhibition activities of handelin were markedly restricted by overexpressing TRAF6 (Fig. 5i), indicating that TRAF6 functions as the axis of Hsp70-targeted anti-inflammatory effect.

Because TRAF6 is an indispensable signal molecule upstream of NF-κB inflammation pathway, we further tested whether handelin could regulate the activation of NF-κB pathway. Immunoblotting assay indicated that PA markedly enhanced the phosphorylation of IKKα/β, I κB-α and NF-κB p65, which was effectively inhibited by handelin treatment in a concentration-dependent fashion (Supplementary Fig. 5e). We also utilized the NF-κB-luciferase reporter gene stably transfected BV2 cells to assess the transcriptional activity of NF-κB, and observed an obviously activated NF-κB-luciferase reporter gene in the presence of PA, which was alleviated by handelin (Supplementary Fig. 5f). Collectively, these results suggest that Hsp70 is required for handelin to inhibit neuroinflammation through regulating TRAF6 polyubiquitination and subsequent NF-κB inflammatory signal.

3.6. Handelin Inhibits Neuroinflammation In Vivo With Fewer Side Effects

To assess the potential effect of handelin for treating neuroinflammatory diseases, we established high fat diet (HFD)-induced neuroinflammation model in vivo (Fig. 6a). Immunoblotting analysis revealed HFD feeding triggered the overexpression of inflammatory proteins including COX-2, TNF-α and IL-β in brain (Fig. 6b). These alternations were effectively reversed by oral administration of handelin (Fig. 6b), suggesting a significant anti-neuroinflammatory effect of handelin. Consistent with these findings, we observed a robust increase of activated microglia in the cortex region of HFD-fed mice, which was indicated by specific ionized calcium binding adaptor molecule-1 (Iba-1) staining (Fig. 6c). Handelin effectively inhibited microglial activation as evidenced by decreasing the number of Iba-1 positive microglia (Fig. 6c). Moreover, we observed similar inhibitory effects of handelin on HFD-induced increases of cluster of differentiation 68 (CD68) and CD11b/c positive microglia (Fig. 6d and Supplementary Fig. 6a). Taken together, these results demonstrated that handelin could suppress HFD-induced microglial activation, as well as the resultant production of inflammatory mediators in brain.

To test whether handelin possesses any possible side effects, we compared the effects of handelin on serum total cholesterol (TC) and routine peripheral blood cells including monocytes, neutrophils, lymphocytes and platelets in BALB/c mice with geranylgeranylacetone (GGA), a classical pharmacological inducer of Hsp70 gene (Fig. 6e). As shown in Fig. 6f, no statistical significant differences were observed between handelin (100 mg/kg/d) and vehicle treatment on monocytes ratio (MONO%), neutrophils ratio (NEUT%) and serum TC level. However, GGA treated-group (100 mg/kg/d) showed markedly elevated serum TC level and MONO% together with a significant reduced NEUT%, which is consistent with the common side effects on clinical trials for GGA. Additionally, both handelin and GGA increased the mean platelet volume (MPV), whereas GGA showed a more significant promotion than handelin (Supplementary Fig. 6b). We further compared the effects of GGA and handelin on PA-induced neuroinflammation via nitrite oxide (NO) assay. Results showed that handelin dose-dependently inhibited NO release, while GGA did not affect NO level at the same concentrations (Supplementary Fig. 6c). These data suggest that handelin might show more advantages over GGA for treating neuroinflammation and maintaining blood fat and peripheral immune function.

Handelin activates Hsp70, which acts as a cellular lifeguard for its multiple biological functions (Jäättelä et al., 1999). In this sense, it may possess positive effects on cell survival and longevity. To test this possibility, we first investigate the effect of handelin on cell injury induced by severe heat stress stimulus. We found that handelin significantly attenuated heat shock-induced SH-SY5Y cell death without affecting the Hsp70 protein expression (Supplementary Fig. 7a and b). We further attempted to access the role of handelin in animal development. We tested the lifespan in *C. elegans* and the survival ratio of early embryonic development in zebrafish. As shown in Supplementary Fig. 7c, *C. elegans* worms fed with 50 μM handelin exhibited an extended longevity compared with the worms fed with *E. coli* OP50 as control (16.85 d in Handlin vs. 14.35 d in Control, an approximately 17% increase in mean lifespan). Moreover, the death ratio was decreased nearly from 20% to 5% by treating with 30 μM handelin for 72 h in the early zebrafish embryo development (Supplementary Fig. 7d). Overall, these results demonstrated the beneficial effect of handelin on cytoprotection and prolongevity.

4. Discussion

Accumulating evidence suggests that abnormal microglial activation in brain is highly associated with neuroinflammation by elevating the expressions of pro-inflammatory cytokines, further leading to neuronal dysfunction and cognitive impairment (Erion et al., 2014; Jeon et al., 2012; Meireles et al., 2015; Miller and Spencer, 2014). Therefore, novel therapy approaches to treat neuroinflammation need to be developed. Here, we used small-molecule handelin as a chemical probe and identified cysteine as a druggable amino acid residue in heat shock protein 70 (Hsp70) against high fat-associated neuroinflammation. We found that handelin significantly triggers Hsp70 activity via directly modifying cysteine 306 (Cys306) in covalent mode. This leads to an allosteric effect on Hsp70 catalytic pocket and promotes the association of Hsp70 with its substrate TRAF6, further blocking TRAF6-dependent neuroinflammation signaling pathway. Therefore, Cys306 may represent a promising drug targeting site on Hsp70 for inhibiting neuroinflammation and resultant neuronal dysfunction.

Hsp70 is highly involved in various neuroimmunological diseases. The induction of Hsp70 (HSPA1A) gene expression (by agent cyclopentenone prostaglandins, heat shock or HSP72 transgene overexpression) shows potential suppressive effects on the products of inflammation-relevant genes (Ding et al., 2001; Ianaro et al., 2003; Liu et al., 2012; Tanaka et al., 2014; Wang et al., 2002). However, direct pharmacological activation of Hsp70 with small-molecules has not been focused for a long time. Here, we found small-molecule handelin significantly inhibits palmic acid-induced microglial activation which is a key milestone for obesity-associated neuroinflammation. Moreover, clear-cut anti-neuroinflammation effects of handelin administration were also evidenced on high fat feeding-induced animal models in vivo.

Target identification of bioactive small-molecules can be extremely fruitful when their target molecules are druggable (Van Eden et al., 2005). Here, we found handelin directly binds to Hsp70 by targeting a previously uncharacterized cysteine residue (Cys306). Remarkably, we demonstrate that handelin covalently modifies Cys306 via the Michael addition reaction, which results in anti-neuroinflammation effect. Current Hsp70-dependent anti-inflammation therapy mainly focuses on promoting endogenous Hsp70 gene expression by genetic approach or chemical inducers (Bianchi et al., 2014; Ding et al., 2001; Ianaro et al.,

2003). However, this strategy suffers from complicated signaling pathway for gene induction and the off-target effect of transcription. Especially, Hsp70 acts as a key hub protein for various physiological functions, thus the inducers of Hsp70 gene expression could disturb several signaling pathways, which cause undesirable side effects. Therefore, direct pharmacological activation of Hsp70 by targeting specific functional amino acid residue can effectively overcome these limitations and provides a more precise regulatory strategy for Hsp70 function with fewer disturbances to the surrounding physiological environment.

Moreover, we demonstrated that handelin selectively activates Hsp70 but not Hsc70 in nanomolar level. We speculate that the corresponding amino acid residue in constitutive Hsc70 is asparagine without highly reactive thiol group, resulting in a loss of covalent binding effect with handelin. This might constitute the structural biology nature of the target selectivity of handelin for different HSP70 subfamily members. It is a remarkable fact that handelin represents a small-molecule that directly activates Hsp70 by targeting cysteine residue to inhibit neuroinflammation.

Hsp70 is found to be highly involved in almost all inflammatory diseases and proposed as a promising target for inflammation therapy (Jian et al., 2016; Van Eden, 2015, Van Eden et al., 2005; Vinokurov et al., 2012). Previous studies reveal that small-molecules could promote ATP hydrolysis process and up-regulate ATPase activity of Hsp70 via allosteric effect (Wang et al., 2016). Handelin promotes ADP release from Hsp70 by inducing allosteric regulation of catalytic pocket in NBD thus facilitates the exchange of ADP and ATP to accelerate ATP hydrolysis cycle. Therefore, handelin-dependent allosteric effect significantly increases ATPase activity of Hsp70, which was confirmed by malachite green and ADP analysis in our study. To our knowledge, this small-molecule-mediated allosteric activation mechanism for Hsp70 has not been reported previously, and allowed the further design and development of novel small-molecule Hsp70 activators in the future.

The formation of lysine63 (K63)-linked poly-ubiquitin chain on TRAF6 is a key cell event for inflammation pathway activation. Previous reports reveal that Hsp70 can directly associate with TRAF6 and block K63-linked polyubiquitination of TRAF6, leading to inactivation of downstream NF-κB inflammatory signal (Chen et al., 2006). In this study, handelin significantly suppresses K63-linked polyubiquitination of TRAF6. We speculate that handelin-dependent allosteric regulation induces the exposure of Hsp70 substrate-binding surface to TRAF6 and facilitates the interaction of Hsp70 with TRAF6. The Hsp70-TRAF6 association further blocks K63-linked polyubiquitination on TRAF6 and inactivates subsequent NF-κB inflammation signaling pathway. Our finding is also supported by previous investigation that Hsp70 inhibits bacterial lipopolysaccharide-induced NF-κB activation by preventing TRAF6 polyubiquitination in macrophages (Chen et al., 2006).

Although GGA, as a typical Hsp70 gene inducer, has been found to show significant inhibitory effect on various preclinical inflammatory models such as colitis or gastritis (Howden, 2014), some outcomes from clinical trials using GGA have questioned its effectiveness and raised potential side effects on gastroduodenal mucosal injury (Kunimoto et al., 2003). We speculated that this might be associated with the allergic reaction caused by GGA-dependent proliferation of monocytes which was observed in our study. However, specific Hsp70 activation by handelin does not induce similar effect on monocyte proliferation, which will result in a more satisfactory availability and adaptability in anti-inflammation drug development. Of course, further investigations need to be carried out.

HSPs are a family of redox sensitive proteins involved in various adverse environmental stressors, including high temperatures (Jäättelä, 1999; Trovato et al., 2016; Vinokurov et al., 2012). Among the HSPs, Hsp70 is extremely prominently encoded by cytoprotective genes called vitagenes to maintain redox homeostasis and cellular repair (Calabrese et al., 2010; Trovato et al., 2016). This idea is strongly supported by the finding that handelin promoted SH-SY5Y cells survival against heat stress-induced cytotoxicity, further confirming the cellular target of handelin as Hsp70. Hsp70 has been reported as a predominant member of vitagene network that exerts protective effect on cells by preventing spontaneous aggregation of toxic misfolding proteins, showing potential effects on anti-aging and longevity (Dattilo et al., 2015; Lanneau et al., 2008). In this work, handelin activated Hsp70 and thereby showed neuroprotection from microglia activation-mediated or heat stress-induced neurotoxicity. Furthermore, we observed that continuous handelin administrations could effectively prolong the lifespan of *C. elegans* and zebrafishes, indicating its anti-aging and longevity activities. However, handelin had no obvious effects on the Hsp70 protein expression. Thus, we speculate handelin exerts cytoprotection by functionally activating Hsp70 rather than regulating the Hsp70 associated-vitagene network. In this context, the vitagene-independent pharmacological activation of Hsp70 protein provides an effective strategy to modulate redox homeostasis and benefit cell survival.

In summary, we firstly reported Cys306 as a druggable residue for direct pharmacological activation of Hsp70, which leads to an effective suppression on neuroinflammation with fewer undesirable side effects. Moreover, small-molecule handelin provides a chemical template for designing specific Hsp70 activators, which presents an important avenue for the development of powerful tool to explore human neuroinflammatory disease.

Acknowledgements

We would like to thank Professor Bao-Lin Liu for helpful discussions and Dr. Jia Li for contributions to the palmitic acid solution preparation. This work was supported by grants from the National Key Technology R & D Program “New Drug Innovation” of China [Nos. 2012ZX09301002-002-002, 2017ZX09101003-008-003]; the Natural Science Foundation of China [No. 81303253].

Competing Financial Interests

The authors declare no competing financial interests.

Author Contributions

K.W. Zeng and P.F. Tu conceived and designed the research. L.C. Wang performed most of the experiments. L.X. Liao and M.X. Song coordinated the experiments. H.N. Lv supported the chemical experiments. D. Liu performed nano-LC-MS/MS analysis. W. Dong and J. Zhu performed *C. elegans* lifespan and Zebrafish embryos development assays. J.F. Chen and M.L. Shi performed the LC-Q-trap-MS analysis. G. Fu coordinated the SPR analysis. K.W. Zeng, P.F. Tu, and L.C. Wang wrote the manuscript.

Appendix A. Supplementary Data

Supplementary data to this article can be found online at http://dx.doi.org/10.1016/j.ebiom.2017.08.011.

References

Alexander, E.K., Vladimir, L.G., 1997. Heat Shock Proteins and Cytoprotection: ATP-deprived Mammalian Cells. Springer.
Bianchi, A., et al., 2014. Oxidative stress-induced expression of HSP70 contributes to the inhibitory effect of 15d-PGJ2 on inducible prostaglandin pathway in chondrocytes. Free Radic. Biol. Med. 76, 114–126.
Calabrese, V., et al., 2010. Oxidative stress, redox homeostasis and cellular stress response in Ménière's disease: role of vitagenes. Neurochem. Res. 35, 2208–2217.
Chen, H., et al., 2006. Hsp70 inhibits lipopolysaccharide-induced NF-κB activation by interacting with TRAF6 and inhibiting its ubiquitination. FEBS Lett. 580, 3145–3152.
Chung, J., et al., 2008. HSP72 protects against obesity-induced insulin resistance. Proc. Natl. Acad. Sci. U. S. A. 105 (5), 1739–1744.
Dattilo, S., et al., 2015. Heat shock proteins and hormesis in the diagnosis and treatment of neurodegenerative diseases. Immun. Ageing 12, 20.

Ding, X.Z., et al., 2001. Over-expression of hsp70 inhibits bacterial lipopolysaccharide-induced production of cytokines in human monocyte-derived macrophages. Cytokine 16, 210–219.
Erion, J.R., et al., 2014. Obesity elicits interleukin 1-mediated deficits in hippocampal synaptic plasticity. J. Neurosci. 34, 2618–2631.
Gething, M.J., Sambrook, J., 1992. Protein folding in the cell. Nature 355, 33–45.
Howden, C.W., 2014. PPI vs. teprenone in preventing recurrence of ulcers during low-dose aspirin. Aliment. Pharmacol. Ther. 40, 1367–1368.
Ianaro, A., et al., 2003. Anti-inflammatory activity of 15-deoxy-delta12,14-PGJ2 and 2-cyclopenten-1-one: role of the heat shock response. Mol. Pharmacol. 64, 85–93.
Jäättelä, M., 1999. Heat shock proteins as cellular lifeguards. Ann. Med. 31, 261–271.
Jeon, B.T., et al., 2012. Resveratrol attenuates obesity-associated peripheral and central inflammation and improves memory deficit in mice fed a high-fat diet. Diabetes 61, 1444–1454.
Jian, J.L., et al., 2016. Progranulin recruits HSP70 to β-glucocerebrosidase and is therapeutic against Gaucher disease. Ebiomedicine 13, 212–224.
Kang, S.S., Kim, J.S., Son, K.H., Lee, C.O., Kim, Y.H., 1996. Isolation of handelin from Chrysanthemum boreale. Arch. Pharm. Res. 19, 406–410.
Kityk, R., Kopp, J., Sinning, I., Mayer, M.P., 2012. Structure and dynamics of the ATP-bound open conformation of Hsp70 chaperones. Mol. Cell 48, 863–874.
Ko, S.K., et al., 2015. A small molecule inhibitor of ATPase activity of HSP70 induces apoptosis and has antitumor activities. Cell Chem. Biol. 22, 391–403.
Kunimoto, S., Murofushi, W., Yamatsu, I., Hasegawa, Y., Sasaki, N., Kobayashi, S., Kobayashi, T., Murofushi, H., Murakami-Murofushi, K., 2003. Cholesteryl glucoside-induced protection against gastric ulcer. Cell Struct. Funct. 28, 179–186.
Lanneau, D., et al., 2008. Heat shock proteins: essential proteins for apoptosis regulation. J. Cell. Mol. Med. 12, 743–761.
Li, J., et al., 2015. Pharmacological activation of AMPK prevents Drp1-mediated mitochondrial fission and alleviates endoplasmic reticulum stress-associated endothelial dysfunction. J. Mol. Cell. Cardiol. 86, 62–74.
Liao, L.X., et al., 2017. Highly selective inhibition of IMPDH2 provides the basis of antineuroinflammation therapy. Proc. Natl. Acad. Sci. U. S. A. 114, E5986–E5994.
Liu, C.X., et al., 2012. Adenanthin targets peroxiredoxin I and II to induce differentiation of leukemic cells. Nat. Chem. Biol. 8, 486–493.
Liu, L., et al., 2014. A sesquiterpene lactone from a medicinal herb inhibits proinflammatory activity of TNF-α by inhibiting ubiquitin-conjugating enzyme UbcH5. Cell Chem. Biol. 21, 1341–1350.
Lomenick, B., Jung, G., Wohlschlegel, J.A., Wohlschlegel, J.A., Huang, J., 2011. Target identification using drug affinity responsive target stability (DARTS). Curr. Protoc. Chem. Biol. 3, 163–180.
Mayer, M.P., 2013. Hsp70 chaperone dynamics and molecular mechanism. Trends Biochem. Sci. 38, 507–514.
Meireles, M., et al., 2015. The impact of chronic blackberry intake on the neuroinflammatory status of rats fed a standard or high-fat diet. J. Nutr. Biochem. 26, 1166–1173.
Miller, A.A., Spencer, S.J., 2014. Obesity and neuroinflammation: a pathway to cognitive impairment. Brain Behav. Immun. 42, 10–21.
Mishima, K., et al., 2015. Lansoprazole upregulates polyubiquitination of the TNF receptor-associated factor 6 and facilitates Runx2-mediated osteoblastogenesis. Ebiomedicine 2, 2046–2061.
Molina, D.M., et al., 2013. Monitoring drug target engagement in cells and tissues using the cellular thermal shift assay. Science 341, 84–87.
Morimoto, R.I., 1998. Regulation of the heat shock transcriptional response: cross talk between a family of heat shock factors, molecular chaperones, and negative regulators. Genes Dev. 12, 3788–3796.
Nilsson, A.M., et al., 2001. Mechanism of the antigen formation of carvone and related α, β-unsaturated ketones. Contact Dermatitis 44, 347–356.
Tanaka, K., et al., 2007. Genetic evidence for a protective role for heat shock factor 1 and heat shock protein 70 against colitis. J. Biol. Chem. 282, 23240–23252.
Tanaka, T., Shibazaki, A., Ono, R., Kaisho, T., 2014. HSP70 mediates degradation of the p65 subunit of nuclear factor κB to inhibit inflammatory signaling. Sci. Signal. 7, ra119.
Trovato, A., et al., 2016. Redox modulation of cellular stress response and lipoxin A4 expression by Coriolus versicolor in rat brain: relevance to Alzheimer's disease pathogenesis. Neurotoxicology 53, 350–358.
Tsan, M.F., Gao, B., 2004. Heat shock protein and innate immunity. Cell. Mol. Immunol. 1, 274–279.
Van Eden, W., 2015. Diet and the anti-inflammatory effect of heat shock proteins. Endocr. Metab. Immune. Disord. Drug Targets 15, 31–36.
Van Eden, W., Van Der Zee, R., Prakken, B., 2005. Heat shock proteins induce T cell regulation of chronic inflammation. Nat. Rev. Immunol. 5, 318–330.
Van Herwijnen, M.J., et al., 2012. Regulatory T cells that recognize a ubiquitous stress-inducible self-antigen are long-lived suppressors of autoimmune arthritis. Proc. Natl. Acad. Sci. U. S. A. 109, 14134–14139.
Van Noort, J.M., 2008. Stress proteins in CNS inflammation. J. Pathol. 214, 267–275.
Vinokurov, M., et al., 2012. Recombinant human Hsp70 protects against lipoteichoic acid-induced inflammation manifestations at the cellular and organismal levels. Cell Stress Chaperones 17, 89–101.
Wang, Y., et al., 2002. Heat shock response inhibits IL-18 expression through the JNK pathway in murine peritoneal macrophages. Biochem. Biophys. Res. Commun. 296, 742–748.
Wang, Y., et al., 2016. Tylophorine analog DCB-3503 inhibited cyclin D1 translation through allosteric regulation of heat shock cognate protein 70. Sci. Rep. 6, 32832.
Wieten, L., et al., 2010. A novel heat-shock protein coinducer boosts stress protein Hsp70 to activate T cell regulation of inflammation in autoimmune arthritis. Arthritis Rheum. 62, 1026–1035.
Yoo, C.G., et al., 2000. Anti-inflammatory effect of heat shock protein induction is related to stabilization of IκBα through preventing IκB kinase activation in respiratory epithelial cells. J. Immunol. 164, 5416–5423.
Yu, A., et al., 2015. Roles of Hsp70s in stress responses of microorganisms, plants, and animals. Biomed. Res. Int. 2015, 1–8.
Zeng, K.W., Zhao, M.B., Ma, Z.Z., Jiang, Y., Tu, P.F., 2012. Protosappanin a inhibits oxidative and nitrative stress via interfering the interaction of transmembrane protein CD14 with Toll-like receptor-4 in lipopolysaccharide-induced BV-2 microglia. Int. Immunopharmacol. 14, 558–569.
Zeng, K.W., et al., 2015. Natural small molecule FMHM inhibits lipopolysaccharide-induced inflammatory response by promoting TRAF6 degradation via K48-linked polyubiquitination. Sci. Rep. 5, 14715.